

Table 2. Listing of compositions of particles A, B and C, in at.%, for elements with $Z \geq 11$

Element	Particle A	Particle B	Particle C
Na	0	2	1
Mg	0	0	1
Al	0	1	5
Si	0	26	57
Ca	0	31	16
Ti	0	20	3
V	0	5	3
Cr	0	2	3
Mn	0	1	1
Fe	37	12	10
Co	63	0	0

rounding of both inclusions and cavities. The rounding of the left-hand and top walls of the cavity can be attributed to this process. Three phases have been satisfactorily identified in this cavity. In the Fig. 7 view, they give distinguishable spatially separated images, labelled A, B and C. The electron-opaque phase A is metallic, B and C are silicates. Table 2 lists the compositions found in A, B and C by EDX (excluding elements with $Z < 11$, which were not detected). The presence of oxygen was confirmed by EELS in both silicate phases. The figures in Table 2 are adjusted for detector sensitivity in the thin-film limit but should be regarded as only semiquantitative.

The phases within cavities were difficult to analyse crystallographically by CBED for several practical reasons. Firstly, the solid angle available for tilting experiments was limited because the beam was shadowed by the adjacent diamond, which thinned more slowly than the inclusion. Further, each cavity usually contained several silicate phases that partially overlapped spatially and were usually strained. Planar and point disorder contributed to the diffuse background. In practice, a microdiffraction technique was used, where a small convergence angle or disc diameter enhanced the contrast

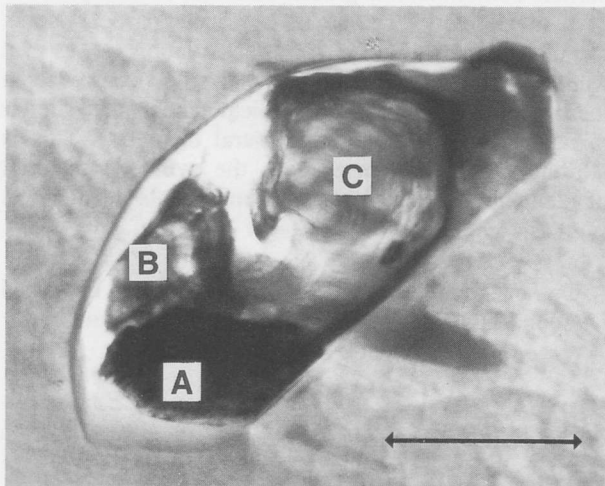


Fig. 7. TEM image of a cavity in diamond containing three identified phases: Fe-Co alloy (A), garnet (B) and a pyroxene (C). Scale mark is 1 μm .

of Bragg reflections relative to the diffuse background. Diffraction patterns were recorded at 250 kV with a probe size of 20 nm. The specimen was cooled to 100 K to reduce the diffuse background and limit radiation damage. Findings concerning particles A, B and C seen in Fig. 7 will now be detailed.

Particle A contained more Co than Fe (Table 2). Diffraction patterns from it were almost impossible to obtain due to the diffuse background. Its images revealed an array of planar boundaries. Similar Fe-Co particles in other inclusions showed patterns consistent with a b.c.c. structure ($a_0 \approx 2.86 \text{ \AA}$). There was no evidence of

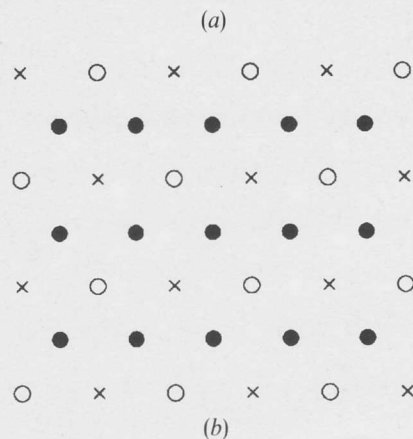
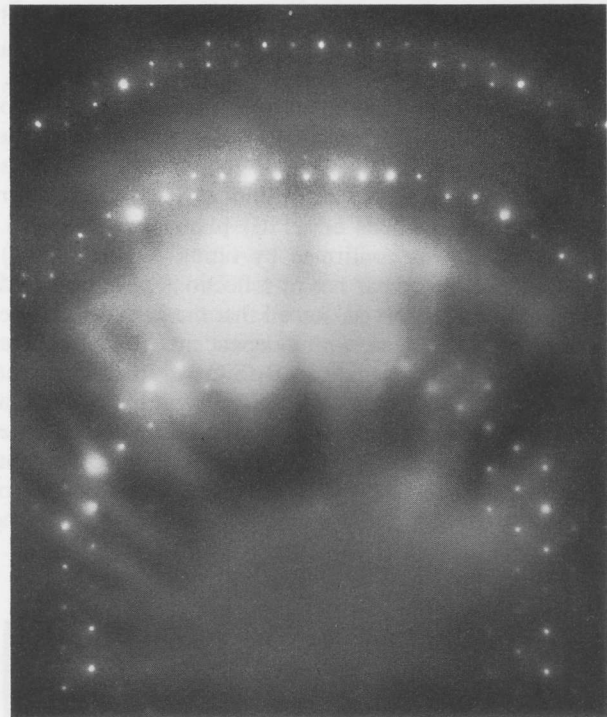


Fig. 8. (a) The $\langle 110 \rangle$ diffraction pattern from the garnet, particle B. (b) Schematic diagram of diffraction geometry. Open circles represent reflections in the zero layer and smaller filled circles show the projected positions of first-order Laue-zone reflections. Crosses represent reflections in the zero layer forbidden by diamond glide planes.